

# GRAPHENE-LIKE STRUCTURED TAP HOLE CLAY FOR LONG LASTING CASTING TIMES AND LOWER CO<sub>2</sub> EMISSIONS

E. Y. Sako\*, D. C. F. Hespanhol, H. D. Orsolini, N. F. Januario, B. M. G. Silva, D. F. Galesi  
Saint-Gobain do Brasil – Performance Ceramics and Refractories - Vinhedo-SP, Brazil

## ABSTRACT

A stable blast-furnace operation is strongly associated with the performance of tap hole clay, which is usually damaged by the combined effect of slag corrosion and pig iron erosion. As such scenario has recently become more challenging due to the use of cheaper raw-materials and low-cost operational practices, Saint-Gobain developed a high-performance solution based on an innovative tap hole clay with a graphene-like structure. Owing to an outstanding chemical resistance and, consequently, a stable and long lasting metal flow, such technology allows operations with reduced fuel consumption, helping to reduce the CO<sub>2</sub> emissions in the ironmaking area.

## INTRODUCTION

The blast-furnace operation is a key step in the steel production chain, as it defines the productivity level of the whole mill. A blast-furnace running with low production level or under unstable conditions will lead to a series of undesired consequences, such as the higher number of torpedo cars out of cycle, an increased demand for steel heating up processes and, more important, a lower final product yield. There are many factors disturbing high productivity operation and one of the most concerning ones is the inefficient drainage of metal and slag, which rises the liquid level and causes instability of blast pressure and burden descent<sup>1</sup>. Tap hole clay plays a role of utmost importance in this scenario, as the flow rate of slag and metal being drained out of the furnace is directly related to the degree of erosion of the tap hole area. Kitamura et al<sup>2</sup> and Youn et al<sup>3</sup> evaluated different tap hole clay formulations, pointing out the best combinations for improved corrosion resistance which could, as a

consequence, lead to a stable pig iron production.

In addition, one must state in mind that, after the implementation of shotcreting for shafts hot repair<sup>4</sup>, the furnace hearth preservation has become the bottleneck for extending the furnace lifetime. That means that besides guaranteeing a suitable flow of liquids, the tap hole clay bears also the task of building and keeping a long and robust mushroom in order to better protect the inner walls around the tap hole<sup>5</sup>. Tsuchiya et al<sup>6</sup> conducted a post-mortem analysis of a blast-furnace after the ending of its campaign and concluded that the tap hole length may change depending on the deadman position, which could consequently affect the mushroom stability.

On the top of that, recent cost-reduction practices applied in blast-furnace operations have significantly affected the standard in-furnace conditions, switching towards a circumferential metal flow and a more aggressive slag chemistry<sup>5,7</sup>. Regular tap hole clays available in the market have been struggling to perform well in such an unfavorable condition, mainly because no breakthrough technology has come up in terms of clay formulation in the past twenty years. The use of Ferron silicon nitride, which initiated in the late 90's, was the last huge technical advance in this product<sup>8</sup>.

Standing out from this stagnation process, Sako et al developed in 2017<sup>9</sup> a novel technology based on a suitable plastic behavior and strong adhesiveness, by combining an optimized grain size distribution and an extremely efficient deflocculant additive. The main target behind that idea was to supply a tap hole clay which was able, firstly, to properly fill in the whole tap hole extension, without any molten metal infiltration or sealing problems,

This UNITECR 2022 paper is an open access article under the terms of the [Creative Commons Attribution License, CC-BY 4.0, which permits](https://creativecommons.org/licenses/by/4.0/) use, distribution, and reproduction in any medium, provided the original work is properly cited.

and then to stick firmly to the hearth wall and to the existing mushroom. Nonetheless, although that was indeed a powerful tool for the hearth walls protection, there was still room for corrosion resistance improvements in order to reach a stable metal production flow.

Carbon sources are usually added in tap hole clay recipes when aiming to decrease the clay wettability to molten metal and slag, and also to develop a strong carbon bonding during sintering<sup>10</sup>. However, the main common added raw-materials are coke, pitch, tar or carbon black, which are comprised only by amorphous phases and do not tend to graphitize very easily. In other words, they fail in achieving a tough and non-wetting microstructure, which explains the above-mentioned ordinary performance of nowadays tap hole clay.

Thus, in order to complement the state-of-the-art hearth walls protection concept and reach the ultimate tap hole clay technology, this work presents an innovative solution for corrosion resistance based on the development of a graphene-like structure. Graphene is worldwide famous for being the first two-dimensional atomic crystal available, comprised of a sheet of sp<sup>2</sup>-hybridized carbon<sup>11</sup> and which provides excellent electrical, optical, chemical, thermal and mechanical properties<sup>12</sup>. Due to such attractive compilation of advantages, graphene has been explored as alternatives for electronics, energy-related systems, sensors and many other applications<sup>13</sup>. Besides all of that, the free-standing layers of graphene's structure tend to stack together through  $\pi$ - $\pi$  and hydrophobic interactions, which leads to a weak basal plane, little structure curvature and the absence of dangling bonds<sup>14,15</sup>. Therefore, chemical reactions on the basal plane of graphene have a large energy barrier, requiring highly reactive species to initiate the reaction, which makes this structure a perfect alternative for tap hole clay, as its refractoriness is extremely high and it could practically not be corroded by neither slag nor molten metal.

In the present work, by adding a new carbon-containing special additive (CCSA) into a state-of-the-art tap hole clay formulation, a graphene-like structure was developed during heating, providing very high mechanical

strength (due to very strong carbon bonding) and excellent corrosion behavior, and guaranteeing an ultimate solution for long lasting casting time. Such stable operations with a smooth liquids drainage might allow blast-furnaces to work with lower fuel consumption and reduced CO<sub>2</sub> footprint.

## MATERIAL AND METHODS

Three compositions were selected to evaluate the formation of the graphene-like structure in the tap hole clay and its possible benefits. All of them present the same overall chemical composition, differing only on the additives contents (Table I). A standard formulation based on the state-of-the-art technology (hereafter denoted as "Standard THM") was used as the base reference and two new compositions were developed by adding the new carbon-containing special additive (CCSA). The new additive was evaluated in two different concentrations: 0,5% and 1%, and the compositions are hereafter denoted as "CCSA THM A and CCSA THM B", respectively.

Table I: Compositions of the evaluated tap hole clays, with different additives contents.

Raw Materials	Compositions		
	Standard THM	CCSA THM A	CCSA THM B
Al <sub>2</sub> O <sub>3</sub>	20	20	20
SiC	21	21	21
Fe-Si <sub>3</sub> N <sub>4</sub>	22	22	22
SiO <sub>2</sub> +Si	19	19	19
C	10	10	10
<u>Carbon-Containing Special Additive</u>	<u>0</u>	<u>0.5</u>	<u>1</u>
Others	8	7.5	7

The FactSage software (FactSageTM6.2; Thermfact and GTT-Technologies, Federal University of São Carlos, FAI, São Carlos, Brazil) was selected to simulate the phase evolution during heating of the tap hole mix with and without the new carbon containing special additive. The calculations of the phases evolution took place at different temperatures: 200°C, 600°C, 1,000°C and 1,400°C at

reducing atmosphere, using Equilib module. FToxid and Fact53 databases were selected for the calculations.

To analyze if the graphene-like structure could be formed in actual laboratory conditions, under the influence of reactions kinetic, X-ray diffraction and Scanning Electron Microscopy using EDS (energy dispersive spectroscopy) spotting analysis were conducted. Samples of Standard THM and CCSA THM B were fired, grounded and sieved through the 325 mesh for the X-ray diffraction analyses. The Standard THM sample was fired at 1,450°C in order to be used as comparative figure of the existing phases, whereas for the CCSA THM B, the spectrum was obtained for samples fired at 400°C, 800°C, 1,000°C and 1,450°C in order to analyze in which temperature de graphene-like structure starts to form. Besides that, one sample of THM with the carbon containing special additive fired at 1,450°C was polished and covered with gold to be analyzed using SEM technique and EDS. The attained results were compared with thermodynamic simulations to better understand the sequence of reactions and its correlation with the results in laboratory evaluation.

The apparent porosity and cold compressive strength were measured according to the NBR 11221/6220 and NBR 11222 standards, respectively. Prismatic samples (160mm x 40mm x 40mm) were obtained by performing the mixing step according to an internal mixing procedure, followed by uniaxial pressing. After pressing, the samples were fired at 800°C, 1,200°C or 1,400°C at reducing atmosphere, cooled down and tested. For the apparent porosity measurement, the samples were immersed in water and boiled for 1 hour to obtain the immersed weight and saturated weigh. The cold compressive strength test was conducted at Universal Testing Machine KRATOS (model: KE-30.000/E MP).

The Hot Modulus of Rupture (HMOR) measurements were carried out according to the ASTM C583 standard under three-point bending tests at 800°C, 1,200°C and 1,400°C. The samples were pressed in a prismatic format (150 mm x 25 mm x 25 mm), pre-fired at their respective test temperature, cooled down, and then reheated during the test, as described in

Figure 1.

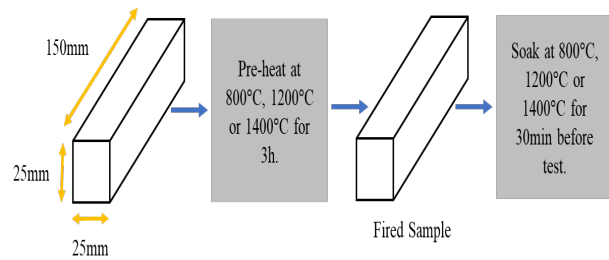


Fig. 1. Description of the sample preparation method for Hot Modulus of Rupture (HMOR) test.

The corrosion tests were conducted in a rotary furnace heated by torch on samples pre-fired at 400°C. The samples' thickness was measured before and after the attack to provide the corrosion resistance index of each formulation. For the slag attack, a 70% slag/30% pig iron mix was used, whereas for the pig iron attack, the mix comprised 80% pig iron and 20% slag. The slag chemical composition is presented at Table II. The corrosion tests took place for two hours around 1,550°C with the slag and pig iron combination changed each hour.

Table II: Chemical composition of the blast-furnace slag used in the corrosion tests.

$SiO_2$	$CaO$	$Al_2O_3$	$Fe_2O_3$	$MgO$	$MnO$	Basicity B2
34	45.5	10.4	0.4	5.5	0.7	1.3

After the lab tests, a pilot trial was conducted in a Brazilian blast furnace (denoted here as BF#A), aiming to validate the better performance of the carbon-containing special additive tap hole mix at field conditions. The blast-furnace produces roughly 7,000 to 8,000 ton of pig iron per day and operates with four tap holes.

## RESULTS AND DISCUSSION

### Graphene-like Structure

Figure 2 shows the thermodynamic simulation for CCSA THM B at reducing atmosphere and different temperatures. The results indicated the likelihood of the graphene-like structure formation in the CCSA

THM B formulation even at very low temperatures, pointing out that such structure is thermodynamically stable and, therefore, its presence in the system is very favorable. Moreover, a rich amount of information can be obtained from this test, such as the phases evolution during the sintering of the tap hole mix. Initially, silicon carbide, silicon nitride, aluminous silicate, carbon, silicon and corundum are observed. At 1,000 °C, aluminous silicate and corundum phases are not present anymore, giving rise to the formation of mullite. Finally, at 1,400°C, an increase in the amount of silicon carbide and a decrease in the amount of free carbon and silicon nitride is observed. It is important to note that the graphene-like structure remains stable at the whole temperature range and that the simulations only considered the thermodynamic barrier for nucleation and growth of a phase. However, when bearing in mind the in situ formation of phases, both the thermodynamic and kinetic barriers must be considered.

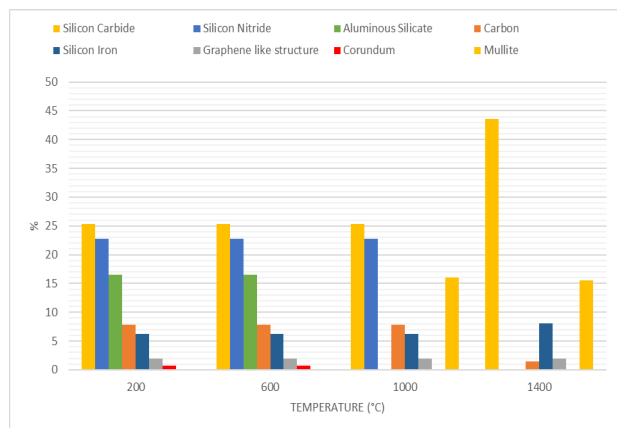


Fig. 2. Thermodynamic simulation results for CCSA THM B, pointing out the phases formed at 200°C, 600°C, 1,000°C and 1,400°C.

Corroborating the thermodynamics calculations, the XRD results showed that the graphene-like phase was indeed formed in the microstructure of the CCSA-containing sample. Figure 3 and Table III depicts the X-ray diffraction spectrum of the (a) Standard THM and (b) CCSA THM B samples. As can be seen, both samples have typical and expected structures for tap hole mixes sintered at 1,450°C, such as aluminous phases, silicon, silicon nitride and silicon carbide, as previously indicated by thermodynamic simulation,

however only the CCSA THM B sample presented the graphene-like structure.

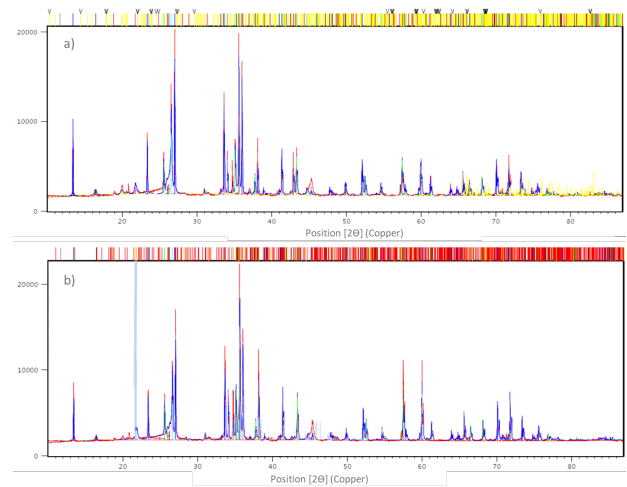


Fig. 3. X-ray diffraction results for a) Standard THM and b) CCSA THM B.

Table III: Description of phases presented at XRD analysis on Figure 3 for Standard THM and CCSA THM B samples.

Formed	Standard THM	CCSA THM B
Silicon Nitride	Present	Present
Aluminum	Present	Present
Silicon	Present	Present
Mullite	Present	Present
Graphite	Present	Present
Silica	Present	Present
Iron	Present	Not present
Graphene-like	Not present	Present

Figure 4 shows a section on the diffraction spectrum of the CCSA THM B sample fired at different temperatures (400°C, 800°C and 1,000°C) in order to highlight the main peak of the graphene-like phase. The sample was analyzed after firing at different temperatures so that it was possible to identify when the formation of the phase in question starts. It can be noted that there is no peak of the graphene-like phase at the lowest temperatures, 400°C and 800°C. Only at 1000°C there seem to be enough temperature and energy for the phase formation.

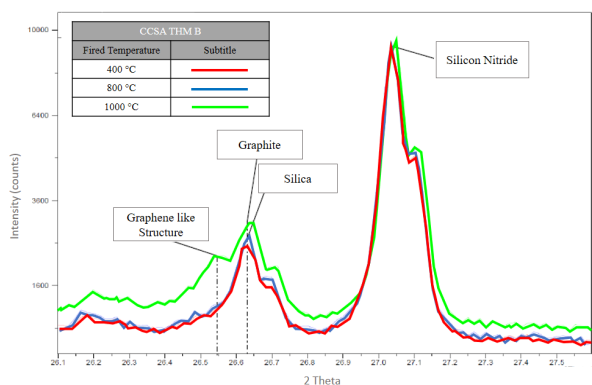


Fig. 4. Specific X-ray diffraction region ( $26.1^\circ \leq 2\theta \leq 27.6^\circ$ ) for CCSA THM B sample, emphasizing the graphene-like phase formation at 1000 °C. The samples fired at 400°C and 800°C did not present such structure.

A lamellar structure typical of the graphene one was identified by Scanning Electron Microscopy (SEM) in the tap hole mix with carbon-containing special additive, as described in Figure 5. This is a very relevant result, as it proves that not only was the graphene-like phase formed, as already verified via the XRD technique, but that the phase was surely generated in the unique 2D-structure which guarantees excellent chemical, thermal and mechanical properties. A comparative analyses of properties at laboratory and field scales will be presented in the next section in order to confirm the better performance which could promote a stable blast furnace operation in the steel industry.

### Benefits behind Graphene-like Structure

Analyzing the results of apparent porosity combined with cold crushing strength of Standard THM, CCSA THM A and CCSA THM B in Figures 6 and 7, it is possible to observe an improvement in the properties of the formulations containing the special additive. At 800°C, despite the similar porosity values of the three materials, the CCSA THM A and CCSA THM B samples presented higher mechanical resistance. At 1,000°C, the CCSA-containing mixes showed higher porosity values, which was, however, accompanied by an increase in mechanical strength. These results are important because it is interesting for the tap hole clay to present

relatively high porosity at intermediate temperatures to allow volatiles to be eliminated during its sintering inside the blast furnace. If there is not enough porosity, the gases generated in the sintering of the clay can generate cracks in the material, harming its performance. At 1,400°C, CCSA THM A and CCSA THM B showed a reduction in apparent porosity when compared to the Standard THM result and again an increase in mechanical strength. At this temperature, it is important that the material presents the lowest porosity level so that its surface area in contact with the pig iron and slag liquids is as small as possible, enhancing its corrosion resistance.

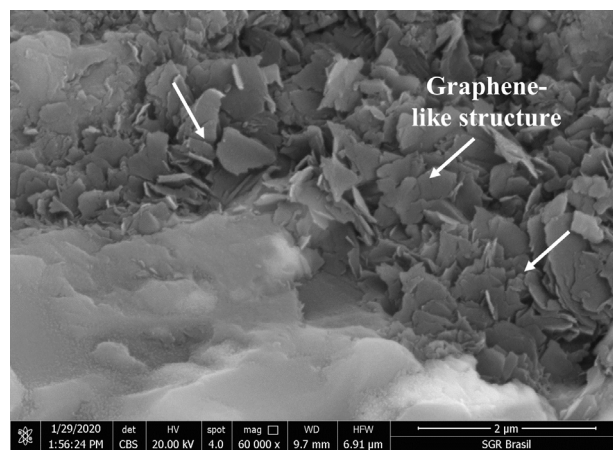


Fig. 5. Scanning Electron Microscopy (SEM) image showing the lamellar structure of the graphene-like phase obtained at CCSA THM fired at 1450 °C.

As CCSA THM A and CCSA THM B samples showed an increase in mechanical resistance at the three evaluated temperatures, there was a suspicion of the formation of glassy phase which could lead to higher cold mechanical strength. As the thermodynamic simulation was not enough, because it did not take into account the impurities that are inherent in refractory raw materials and could result in the formation of liquid phases, hot modulus of rupture was measured for the three samples at different temperatures (800°C, 1,200°C and 1,400°C). From the results present in Figure 8, it is clear that the better mechanical behavior is due to the presence of the graphene-like phase, with no relation to any liquid phase. The CCSA-containing samples showed the highest values of HMOR at the

whole temperature range, with CCSA THM B showing the best result of hot mechanical resistance at 1,400°C.

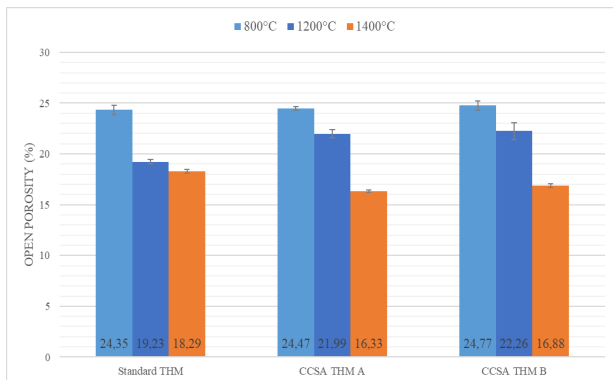


Fig. 6. Open Porosity (%) of the evaluated materials after heat-treatment at 800°C, 1,200°C and 1,400°C.

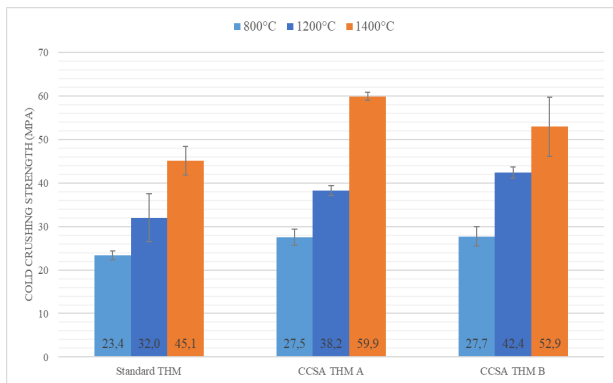


Fig. 7. Cold crushing strength (MPa) of the evaluated materials after heat-treatment at 800°C, 1,200°C and 1,400°C.

The better hot mechanical behavior and the reduced porosity values, as well as the low wettability features of the graphene-like structure, are favorable aspects for achieving an increased corrosion resistance. Figure 9 presents the wear resistance after slag and pig iron attack in a rotary furnace for the three evaluated compositions, with results being relative to the Standard THM sample. It is straightforward to notice the benefits of the low reactivity of the graphene-like phase, reducing the interaction with both slag and pig iron and, as a consequence, decreasing the wear of CCSA THM A and CCSA THM B samples. In fact, CCSA THM B showed an outstanding performance, with roughly 20% reduction on the slag corrosion, which is directly related to the higher content of the carbon containing special additive present in its formulation.

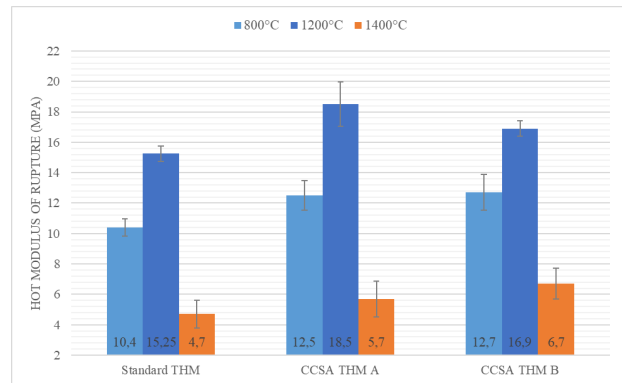


Fig. 8. Hot modulus of rupture (MPa) values for “Standard THM”, “CCSA THM A” and “CCSA THM B” samples attained at 800°C, 1,200°C and 1,400°C.

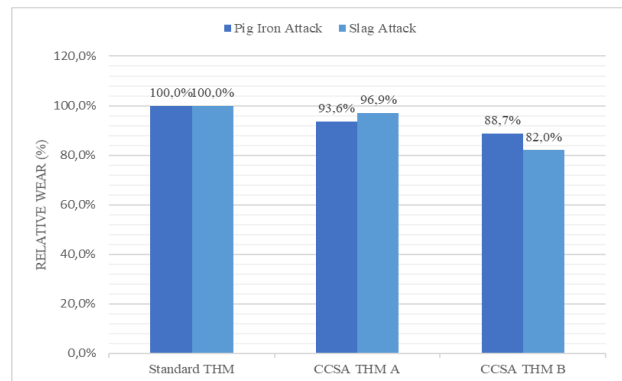


Fig. 9. Wear resistance after slag and pig iron attack for the three evaluated compositions. The results are expressed in a relative index, considering the Standard THM as the reference.

Such results confirmed in lab scale that the generation of a graphene-like structure could be a breakthrough advance into long lasting casting time formulations for high performance tap hole clay. Based on this positive scenario, a large industrial production of CCSA THM B formulation was conducted in order to verify the potential better performance at a field trial. The clay was produced without any change on process parameters and the material was tested at a blast-furnace producing 7,000 t of pig iron per day (BF #A) in a large Brazilian steel mill. Figure 10 highlights the casting time of CCSA THM B formulation, comparing to the standard THM clay which was used right before. One can observe that just after a few castings the composition containing the novel technology was able to significantly enhance the casting time, moving the average value up to 50% more than the ones attained by the standard material.

Besides assuring a continuous and stable drainage of liquids, the new tap hole clay could also provide a reduction in the carbon footprint consumption by better controlling the input of carbon-containing fuels.

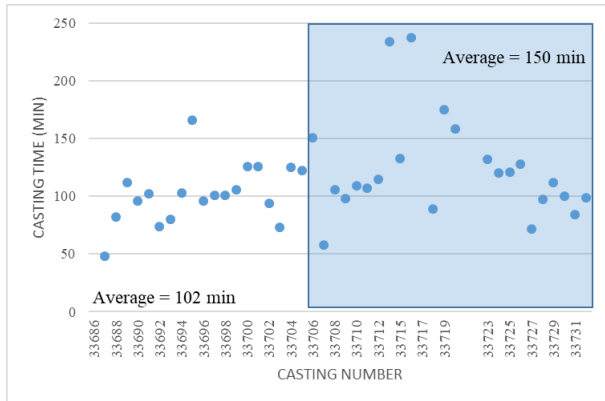


Fig. 10. Casting time of CCSA THM B formulation (highlighted inside the blue square) when used at BF#A, compared to the Standard THM clay which was used right before.

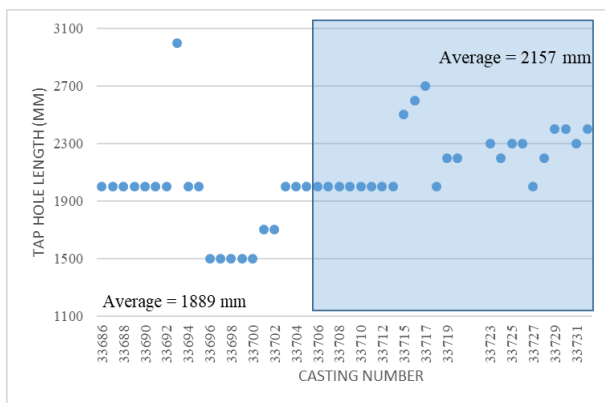


Fig. 11. Tap hole length of CCSA THM B formulation (highlighted inside the blue square) when used at BF#A, compared to the Standard THM clay which was used right before.

A relevant increase in the tap hole length values was also observed as an additional benefit during the field trial, as displayed in Figure 11. Due to a lower wear degree, the clay mushroom inside the furnace was kept undamaged and the average tap hole length values increased roughly 15%. Differently from the casting time, however, it takes some time for the new clay to replace the old material and build a new and tough mushroom, which better protects the hearth walls and prevent them to wear out through the remaining campaign.

## CONCLUSIONS

An ultimate tap hole clay technology was presented in this work, based on the introduction of a graphene-like structure by adding a carbon containing special additive, which was able to provide excellent chemical, thermal and mechanical properties. Thermodynamic calculations and microstructural analyses showed the stability of such phase in the tap hole clay structure, whereas laboratory tests confirmed its main benefits: higher mechanical strength, reduced open porosity and enhanced corrosion resistance (during both slag and pig iron attack).

The pilot trial at a large blast-furnace pointed out that the excellent properties of the novel tap hole clay observed in the laboratory were responsible for making the furnace operate with long lasting casting times, leading, consequently, to a potential reduction on fuel consumption. A better protection of the hearth walls could also be observed, due to longer tap hole length values. Both results evidenced the breakthrough advance brought by this novel technology, which was able to keep high performance even during the current scenario of constant changing of operational conditions.

## REFERENCES

1. T. Nouchi, M. Sato, K. Takeda, T. Ariyama, "Effect of operation condition and casting strategy on drainage efficiency of the blast-furnace hearth", *ISIJ International*, 45 [10] 1515-1520 (2005).
2. M. Kitamura, R. Nakamura, H. Sumimura, "Study of the high density tap hole clay for blast furnace", *Journal of the Technical Association of Refractories, Japan*, 22 [4] 350-354 (2002).
3. S. Youn, K. Kim, M. Choi, "Development and application of high  $Al_2O_3$  tap hole clays for blast-furnace", *Unitecr 97 Proceedings*, pp 693-704 (1997).
4. G. H. Gronebaum, J. Pischke, "Investigation on shot-cast mixes for blast-furnace relining", *Steel Research International*, 80 [11] 808-815 (2010).

5. K. Spaleck, M. Schoeman, W. Seegers, et al., "Practices and design for extending the hearth life in the Mittal Steel Company blast furnaces", Fifth European Coke and Ironmaking Congress, Stockholm, Sweden, pp 10-15 (2005).
6. N. Tsuchiya, T. Fukutake, Y. Yamauchi, T. Matsumoto, "In-furnace conditions as prerequisites for proper use and design of mud to control blast-furnace tap hole length", ISIJ International, 38 [2] 116-125 (1998).
7. R. J. van Laar et al., "Blast furnace hearth management for safe and long campaigns", Iron and Steelmaking Technology Conference Proc, Indianapolis, Indiana, pp 1079–1090 (2003).
8. K. Kometami, K. Iizuka, T. Kaga, "Behavior of ferron-Si<sub>3</sub>N<sub>4</sub> in blast furnace tap hole mud", Taikabutsu Overseas, 19 [1] 11- 14 (1999).
9. E. Y. Sako et al, "High performance taphole clay: a key for blast furnace hearth protection and a tool for cost reduction", Iron and Steel technology, pp 82-87 (2018).
10. K. Masatsugu, N. Ryosuke, K. Toshihiko, S. Hisaki, K. Tatsuya, "Development of high durability tap hole mix for blast furnace", Unitecr 99 Proceedings, pp 59-61 (1999).
11. K. S. Novoselov, V. I. Falko, L. Colombo, P. R. Gellert, M. G. Schwab, K. Kim, "A roadmap for graphene", Nature Research, 490 [11] 92-200 (2012).
12. M. J. Allen, V. C. Tung, R. B. Kaner, "Honeycomb carbon: a review of graphene", Chemical Reviews, 110 [1] 132-145 (2010).
13. K. Rana, J. Singh, J. Ahn, "A graphene-based transparent electrode for use in flexible optoelectronic devices", Journal of Materials Chemistry C, pp 2646-2656 (2014).
14. A. Fasolino, J. H. Los, M. I. Katsnelson, "Intrinsic ripples in Graphene", 6 [11] 858-861 (2007).
15. L. Yan et al, "Chemistry and physics of a single atomic layer: strategies and challenges for functionalization of graphene and graphene-based materials", Chem. Soc. Rev., 41 [1] 97-114 (2011).